

FORECASTER: A Continual Lifelong Learning Approach to Improve Hardware Efficiency

Phat Nguyen¹, Abhishek Taur¹, Abdullah Muzahid¹, Arnav Kansal², and Mohamed Zahran²

¹Department of Computer Science and Engineering, Texas A&M University

²Department of Computer Science, New York University

ABSTRACT

Computer applications are continuously evolving. However, significant knowledge can be harvested from older applications or versions and applied in the context of newer applications or versions. Such a vision can be realized with *Continual Lifelong Learning*. Therefore, we propose to employ continual lifelong learning to dynamically tune hardware configurations based on application’s behavior. The goal of such tuning is to maximize hardware efficiency (i.e., maximize an application’s performance while minimizing the hardware’s energy consumption). Our proposed approach, FORECASTER, uses deep reinforcement learning to continually learn during the execution of an application as well as propagate and utilize the accumulated knowledge during subsequent executions of the same or new application. We propose a novel hardware and ISA support to implement deep reinforcement learning. We implement FORECASTER and compare its performance against prior learning-based hardware reconfiguration approaches. Our results show that FORECASTER can save as much as 17.5% system power over the baseline set up with all resources. On average, FORECASTER saves 16% system power over the baseline setup while sacrificing an average of 4.7% of execution time.

1. INTRODUCTION

Computer architects are in continuous quest to find the best hardware design for different program types. We cannot have different application specific hardware designs for different program types because this will be prohibitively expensive. What makes things even more challenging is that a single program passes through different phases during its execution lifetime and each phase has a different *best* hardware configuration. This paper presents a step toward a solution.

Previously, designers used to gather profiling information about a program execution on a hardware, then make use of this profiling information to either enhance the hardware or the program. However, this means that each program must be instrumented first and the information gathered during profiling is used on that application only. Our proposed idea is based on a simple hypothesis: any phase of a program execution has a best hardware configuration. Each phase has certain characteristics. So, if there is a different program with a phase with similar characteristics, then it can use the same configuration to get the best performance. Therefore, if we can *learn* the best configuration for different program phases,

we can use that to get the best configuration for new, unseen, programs. In other word, there is a finite set of patterns along which hardware/software interactions can occur to give best performance. For example, given a cache configuration, there are finite set of memory access patterns that yield low cache misses. Or, given a memory access pattern, we can build the best cache configuration that yields the lowest number of misses. **The main goal of this paper is to design a hardware with configurable knobs that learns from its interaction with programs to be able to reconfigure itself to a configuration that achieves best performance for new unseen programs.** As the hardware executes more programs, it learns more patterns and can achieve better performance for more and more programs.

There are several challenges that need to be tackled in order to reach this goal. First, what are the knobs to be changed? There are many structures that can be designed to be reconfigurable. Our main criteria is to pick knobs that have the biggest impact on performance and power and at the same time can be reconfigured with the least hardware cost and modification. Second, how to learn the patterns of the hardware/software interaction to suggest the best configuration? The pattern means the profiling information such as telemetry collected from performance counters. For each pattern, there is a hardware configuration that leads to the best performance and power, or any other metric that needs to be optimized. It is clear that the number of patterns is large and, depending on the number of type of knobs, the hardware configurations is also large. This is why straightforward classifiers such as bloom filter may not be a viable option. Using neural network in a deep-learning setup does not lead to best results from an early stage because it requires a large number of examples in the training phase. Therefore, we need some kind of unsupervised learning approach. We read profiling information and we make changes to the hardware based on this information. That is, we make changes to the environment and we get feedback about how well we do. This is a description of reinforcement learning.

The main contribution of this paper is to propose a hardware scheme, called FORECASTER, that uses continuous learning, from one execution to another, using a deep reinforcement learning to reconfigure certain knobs to get the best performance and power for different programs. We implemented FORECASTER using Multi2Sim [32] simulator. Our experimental results using Parsec benchmarks show that the proposed technique can save as much as 17.5%

power over the baseline with all resources. On average, our scheme saves 16% system power over the baseline setup while sacrificing only an average of 4.7% execution time.

The rest of the paper is organized as follows: Section 2 presents some background materials; Section 3 describes the main idea of FORECASTER; Section 4 shows the detailed implementation of FORECASTER; Section 5 presents some experimental results; Section 6 highlights some related work; and finally, Section 7 concludes our work.

2. BACKGROUND

2.1 Hardware Adaptation

There is a considerable amount of prior work on reconfigurable architecture [3, 4, 8, 21, 33]. However, unlike FORECASTER, the majority of the work did not use any learning [3, 21]. Among the learning-based approaches, most used offline training [4, 8, 33]. Only a few approaches utilized online training; however, they focused on a single hardware structure [12].

Choi and Yeung [6] perform microarchitectural resources distribution in an SMT processor using hill-climbing algorithm. Bitirgen et al. [4] propose a scheme to combine performance prediction model of multiple applications to get an aggregate performance prediction of the overall resource distribution. The scheme is coupled with some limited probabilistic search technique to find the optimal resource distribution to improve performance. Petrica et al. [21] present Flicker, a general-purpose multicore architecture that dynamically adapts to varying limits on allocated power. A Flicker core has reconfigurable lanes through the pipeline that allows tailoring an individual core to the running application with lower overhead.

Dubach et al. [8] propose the use of machine learning to dynamically optimize the efficiency of some processor’s components such as the Arithmetic Logic Unit, instruction queues, register file, caches, branch predictor, and the pipeline depth. During program execution, as soon as a phase change is detected, the hardware starts to collect counters on a predefined profiling configuration. These counters represent the usage of the hardware resources in that interval. The model then predicts the optimal configuration and the system is reconfigured accordingly for the rest of the phase. Unlike our approach, Dubach et al. proposes learning for each program separately. Moreover, they also use the offline training method, which could limit the adaptability of the model to future unmet programs.

There is also some other work in utilizing profiling information for optimization. However, majority of the work is related to software optimization [19]. For hardware designs, profiling information has been traditionally used to make design choices for hardware before fabrication [11].

2.2 Reinforcement Learning

2.2.1 Overview

Reinforcement learning is a subset area of machine learning concerned with autonomous agents that can learn without supervision to optimize an objective [10]. In reinforcement learning, the knowledge of the agent is built through trial

and error. For each time step, the agent takes an action and observes feedback from the environment about how good it is doing and how close it is to the goal. A reinforcement learning problem typically consists of three main components:

- a set of *states* that represent the environment at different time steps;
- a set of possible *actions* that the agent can take;
- a *reward function* that issues a reward for each action of the agent

A *state* is defined as the information about the condition of the environment at a time step. The agent observes this information and selects the most appropriate *action*. As the agent taking the selected action, the environment transitions from the current state to another state. After that, the *reward function* assigns the agent with a reward. The value of this reward depends on how good the state-action pair is. Since the name of this reward function is Q – *function*, the reward is called Q – *value*. The agent accumulates the knowledge by storing and updating these Q-values after each time step.

Ipek et al. [12] formulate DRAM scheduling as a reinforcement Q-learning problem with the goal of optimizing bus utilization and throughput. In every clock cycle, the agent picks one out six possible actions available to the scheduler. The agent is given a numerical Q-value of 1 whenever it issues a command that increases the data bus utilization and 0 otherwise. The state is defined as a combination of attributes that represent the state of the controller’s transaction queue. Ipek et al. show that this approach can improve the bus utilization and bandwidth efficiency by a significant amount compared to the state-of-the-art DRAM scheduler.

2.2.2 Deep Q-learning

Early reinforcement Q-learning techniques use a Q-table to store the Q-values and take the state-action pairs as the indices. As modern problems getting more and more complex, this approach become inefficient since the Q-table size inflates with the number of state-action pairs. The answer to this issue is Deep Q-learning (DQN), which is the cross breeding of reinforcement Q-learning and deep learning techniques. In DQN, the reward table is replaced by a multi-layer neural network that predicts the Q-value for any particular state-action pair.

There are a significant amount of work on the application of DQN [17, 27, 28, 29]. Mnih et al. [17] apply DQN to seven 2600 Atari games and show that it outperforms all previous reinforcement learning approaches. Moreover, this DQN model also manages to beat a human expert in three out of seven games. The model uses only the raw pixels of the application screen as input, and outputs the expected future reward of the taken action. DeepMind Technologies uses DQN in the series of AlphaGo programs [27, 28, 29] to solve the game Go. The original AlphaGo version [27] outperforms all previous Go programs and is the first Go program to beat a professional human player. The latest version of the series, AlphaZero, has the capability of teaching itself three different games: Go, chess, and shogi [28]. However, at the time of this paper, there has not any published research on applying DQN in hardware optimization.

3. MAIN IDEA: FORECASTER

FORECASTER periodically collects hardware telemetry during the execution of a program. The telemetry consists of various hardware event counters maintained by the processor architecture. FORECASTER uses the hardware telemetry in a deep reinforcement learning algorithm to predict the optimal configurations of tunable hardware resources. The goal of the predicted configurations is to maximize the efficiency of the hardware. The overall workflow of FORECASTER is shown in Figure 1. FORECASTER reconfigures the hardware resources according to the prediction and receives a reward after a while. FORECASTER receives a positive reward if the hardware efficiency improves due to reconfiguration. Otherwise, it receives a zero or negative reward. Rewards are a feedback mechanism to encourage configurations associated with positive rewards while discouraging non-positive reward related configurations. Based on the reward, FORECASTER updates the Q-values (used by the reinforcement learning algorithm) so that efficiency boosting configurations are predicted more frequently. Thus, FORECASTER continually improves its prediction during the execution of an application. Next time, the same or a new application executes, FORECASTER reuses the Q-values learned from prior executions and continues to improve its prediction accuracy. In other words, FORECASTER keeps on learning from one execution to the next both within and across applications, thereby realizing continual lifelong learning with the goal of maximizing the hardware efficiency. In the next few sections, we will elaborate on different steps of FORECASTER.

3.1 Initial Configuration

When an application starts, FORECASTER starts with maximum amount of hardware resources. This prevents any slow down from the beginning. Progressively, FORECASTER tries to reconfigure tunable hardware resources to maximize the hardware efficiency. We used $IPC^3/Power$ as the metric for hardware efficiency. Similar metric has been used in prior work [8]. As for tunable hardware resources, we choose L2 and L3 caches as well as the Branch Target Buffer (BTB) and prefetcher. We choose caches because they are the most energy hungry resources in a chip [13]. We choose the other resources because they can be easily clock-gated without intrusive changes to the pipeline circuitry. Although we demonstrate the effectiveness of FORECASTER with these 4 tunable resources, we argue that FORECASTER is general enough to accommodate any number of tunable resources. Table 1 shows the tunable resources and possible configurations.

Tunable Resource	Configuration
BTB Size	0.5K, 1K, 1.5K, and 2K Entries
Prefetcher	On , Off
L2 (private) cache	256K, 512K, 768K, and 1024K Bytes
L3 (shared LLC) cache	4M, 8M, 12M, and 16M Bytes

Table 1: List of tunable hardware resources. Initial configuration is shown in bold-faced.

3.2 Collecting HW Telemetry and Making Predictions

A program usually goes through distinct phases during its execution [25]. Some phases may benefit from more caches while others might benefit from having a larger BTB. We collect hardware telemetry as an approximation of how a program behaves. Modern processors provide hundreds of hardware event counters as its telemetry. After inspecting every hardware event counter, we choose n counters most relevant to the tunable hardware resources. Let us denote the set of counters (i.e., hardware telemetry) as $\mathbb{T} = \{T_i\}_{i=1}^n$, where each T_i is an individual counter. FORECASTER collects these counters at a regular interval. At the beginning of each interval, FORECASTER uses the counters for predicting configurations of tunable resources.

FORECASTER uses reinforcement learning, more specifically Deep Q-learning (DQN) model for prediction. In this model, the current configuration of the hardware resources, \mathbb{C} , as well as the behavior of the program as specified by the telemetry, \mathbb{T} , is provided as a state, \mathbb{S} . In other words, $\mathbb{S} = \langle \mathbb{T}, \mathbb{C} \rangle$. Given a state, \mathbb{S}_t , at a time period, t , the deep Q-learning model predicts Q-values for all possible actions in that state using a deep neural network (DNN). Each action indicates a different configuration of the hardware resources. Thus, if we have N possible actions, the model predicts N different Q-values - one for each action, A_i , where $1 \leq i \leq N$. The Q-value associated with action A_i , say Q_{A_i} , is an estimation of how good the new configuration (corresponding to A_i) is in maximizing the hardware efficiency. Higher Q-value implies better configuration. Therefore, FORECASTER chooses the action related to the maximum Q-value.

Naively designating one action for each configuration leads to a large number of actions. For example, based on Table 1, we can have $4*4*2*4=128$ possible configurations and hence, the same number of actions. Reinforcement learning with a large action space takes a long time to train due to the sparsity of rewards [24]. Therefore, in order to reduce the number of actions, we express each action in terms of the changes in configurations. Suppose, \uparrow , \downarrow , and $=$ indicate that a resource should be increased, decreased or kept at the same level respectively. If a resource has only two configurations, we can use *ON* and *OF* to indicate those configurations. With these notations, we can define an action as $A = \langle R_a^i \rangle_{i=1}^n$, where R^i represents i -th resource for $1 \leq i \leq n$ and a represents a change in R^i 's configuration such as $\uparrow, \downarrow, =, ON$, or *OF*. For example, suppose the current configuration is denoted by $C = \langle L2_{512}, L3_8, PF_{OF}, BTB_{0.5} \rangle$. Then, an action $\langle L2_{\uparrow}, L3_{\downarrow}, PF_{OF}, BTB_{\uparrow} \rangle$ will create a new configuration denoted by $\langle L2_{768}, L3_4, PF_{OF}, BTB_1 \rangle$. With this new approach, the number of actions is reduced from 128 to $3*3*2*3=54$ i.e., less than half of the initial actions. With the reduced action space, the overall prediction process is illustrated in Figure 2.

3.3 Reconfiguring HW Resources

FORECASTER reconfigures the tunable resources according to the predicted configurations. Now, we describe how each resource is reconfigured.

3.3.1 Branch Target Buffer (BTB)

BTB has 4 possible configurations (Table 1). Therefore, we can partition BTB into 4 sections - B_1 , B_2 , B_3 , and B_4

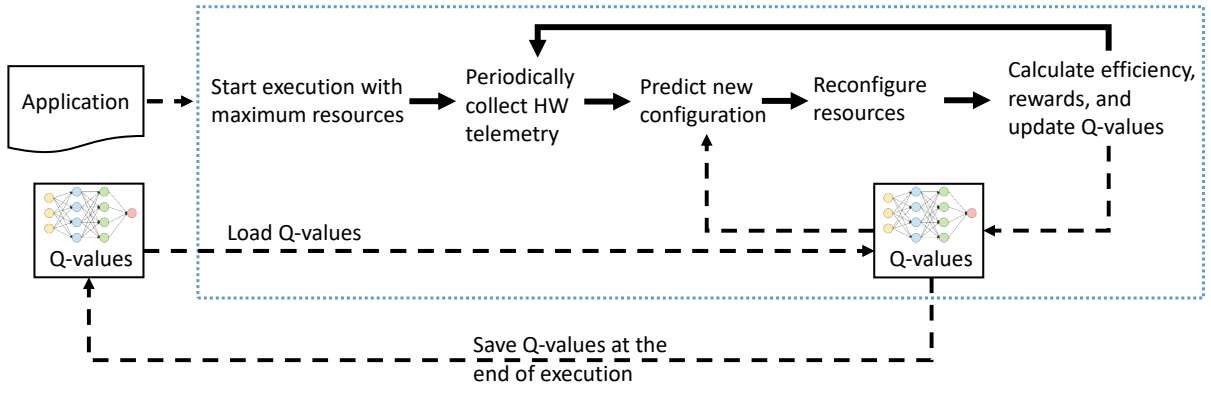


Figure 1: Overall workflow of FORECASTER.

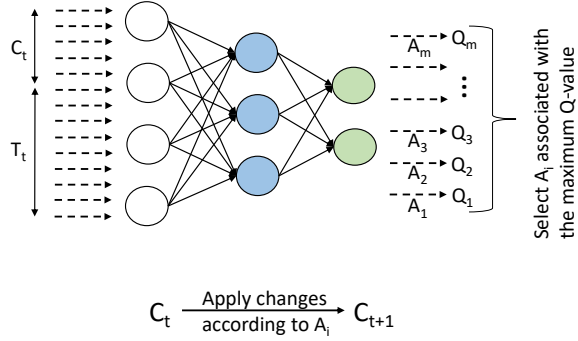


Figure 2: FORECASTER uses hardware telemetry to predict configurations.

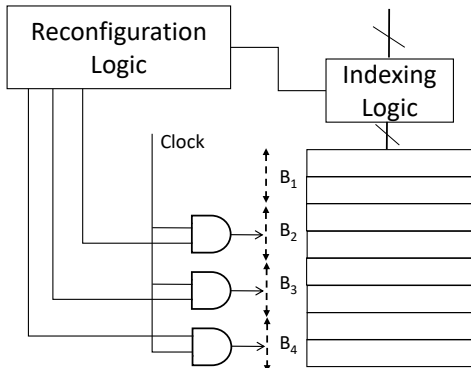


Figure 3: Logic for reconfiguring the BTB.

(Figure 3). For the first configuration (i.e., 0.5K entries), sections (B_2 , B_3 , B_4) are clock-gated. Similarly, for the second and third configurations, sections (B_3 , B_4) and (B_4) are clock-gated respectively. The last configuration does not clock-gate any section at all. On the other hand, Section B_1 is never clock-gated because at least those entries in BTB are used in all configurations. We add a reconfiguration logic that creates the appropriate clock-gating signal to enable the appropriate sections. Moreover, for each configuration, the indexing logic needs to reconfigure the indexing bits accordingly. In a multicore processor with one BTB per core, FORECASTER reconfigures all BTBs to the same configuration. This is done to simplify the prediction and reconfiguration logic in FORECASTER.

3.3.2 Prefetcher

Prefetcher is used either completely or not at all. Therefore, the prefetcher is clock-gated entirely or not at all. So, the reconfiguration logic simply generates a single clock-gating signal for the entire prefetcher.

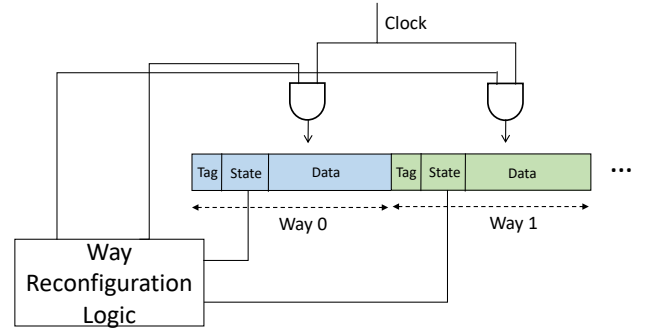


Figure 4: Logic for reconfiguring L2 and L3 caches.

3.3.3 L2 and L3 Caches

In order to reconfigure caches, FORECASTER makes three design choices. *First*, FORECASTER does not clock-gate an entire set. As a result, the address decoding logic remains unchanged. *Second*, from each set, FORECASTER clock-gates the invalid lines. FORECASTER never clock-gates any valid lines from the cache. *Three*, whenever more than the required

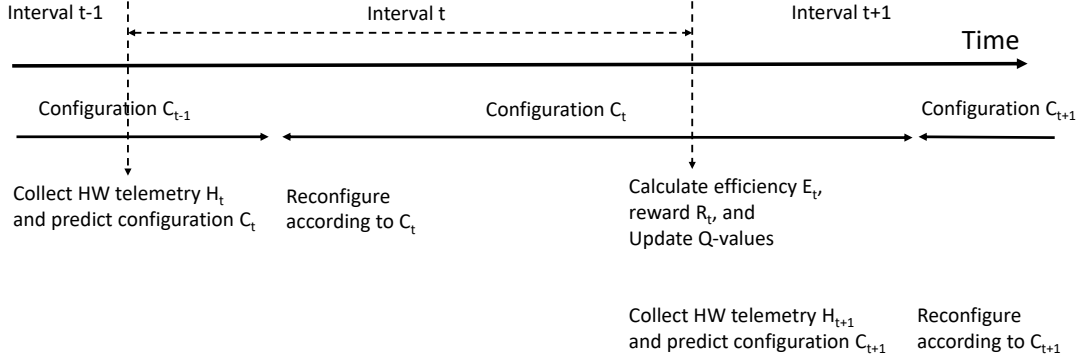


Figure 5: Timing of various steps of FORECASTER.

number of cache lines in a single set satisfy the selection criteria, FORECASTER randomly choose some of them to clock-gate. Figure 4 shows the schematic for reconfiguring the caches. The way selection logic first determines how many lines need to be clock-gated in each set. Then, it selects which way to clock-gate based on the selection criteria and then, sends a signal to that way. When an invalid line is clock-gated, FORECASTER does not need to worry about cache coherence issues. During the clock-gating process, the cache controller blocks any incoming request to that particular cache set. The request is handled after the clock-gating is complete.

3.4 Calculating Rewards and Updating Q-values

FORECASTER collects the hardware telemetry, H_t at the beginning of an interval, t , and determines the new configuration, C_t , using the Q-value, Q_t , predicted by DNN. Then, it reconfigures the hardware resources accordingly, and continues the program execution. The timing is shown in Figure 5. At the beginning of the next interval, $t+1$, FORECASTER calculates the new efficiency that results from the reconfiguration. FORECASTER compares the new efficiency with the old one (the one calculated at the beginning of interval t). If efficiency increases, FORECASTER receives $+1$ reward. If the efficiency remains unchanged FORECASTER received 0 reward. On the other hand, if the efficiency decreases, FORECASTER receives -1 reward. Based on the reward, FORECASTER uses the commonly used temporal difference method to update Q_{t-1} (the Q-value predicted at interval $t-1$) [30]. In this method, the new Q-value, Q'_{t-1} is calculated using the following equation:

$$Q'_{t-1} = (1 - \alpha)Q_{t-1} + \alpha[r + \gamma Q_t]$$

Here, α is the learning rate and γ is the discounted factor. The DNN uses back propagation method to learn Q'_{t-1} .

3.5 Continual Lifelong Learning

Use of DQN in FORECASTER provides a natural way to implement continual lifelong learning. In the DQN model, FORECASTER learns by training a DNN with Q-values. To continue learning from one execution to the next, FORECASTER stores the DNN topology and weights in a file at the end of each execution. Section 4 presents an extension to the

ISA that is used to read the topology and weights of the DNN and write them back in a special file. At the beginning of the next execution, FORECASTER loads the topology and weights of the DNN and continues to learn from where it left in the last execution. If multiple applications are concurrently running in a processor, each application will store its own DNN topology and weights at the end of the respective execution. In that case, FORECASTER uses an offline process to merge the networks periodically (e.g., once a day). For merging, FORECASTER uses TensorFlow [1] to load all the DNNs, and generates a number of random state samples. For each state sample, FORECASTER calculates the Q-value of each action using all the DNNs, takes an average of the Q-values, and retrain the largest DNN. Thus, the largest DNN accumulates the knowledge of all DNNs. During the beginning of the next execution of an application, FORECASTER loads this DNN and continues execution.

4. IMPLEMENTATION

In this section, we outline the implementation of Deep Q-Learning in FORECASTER as well as the extension to the ISA.

4.1 Deep Q-Learning (DQN) Module

We propose to add a DQN module in the chip. The module contains a Neural Processing Unit (NPU) for implementing the DNN along with additional buffers such as input and replay buffers, and a control logic. Figure 6 shows the high level schematic of the DQN module.

There are several NPU designs in literature [2, 9, 23]. We propose to use an NPU similar to the one proposed by Esmaeilzadeh et al. [9]. It consists of a number of Processing Elements (PEs) and a scheduler. Each PE implements an individual artificial neuron. Each PE contains input and weight registers, a multiplier, an adder, a partial sum register, and a comparator. Input and weight registers along with the adder, multiplier and partial sum register are used to calculate the dot product of inputs and weights. The comparator is used to implement ReLU activation function [18]. The scheduler schedules each layer of the DNN in the PEs starting from the input layer. After calculating the Q-values, the current input and Q-values are stored in the replay buffer. When FORECASTER receives a reward and calculates the updated Q-value, the replay buffer provides the saved inputs and Q-values to the

NPU to learn the new Q-value.

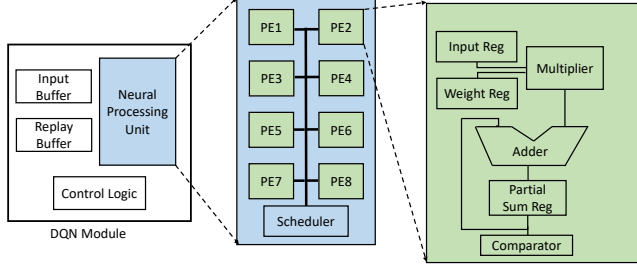


Figure 6: Details of the DQN module.

The control logic sequences the operations to implement the DQN algorithm. The control logic also contains three special registers to store learning rate, discount factor and exploration ratio. The learning rate and discount factor are used to calculate new Q-value (Section 3.4). Exploration ratio dictates how many times the module will choose a random exploratory action as opposed to an action based on the maximum Q-value. DQN uses exploratory action to explore actions that would have been otherwise never selected. This is done to find a potentially better action than the one based on prior knowledge.

4.2 Communicating Telemetry and Reconfiguration Decision

Based on our experiments (Section 5.2.6) and intuition, we select the following hardware counters as telemetry - (i) number of integer instructions, (ii) number of logical instructions, (iii) number of floating point instructions, (iv) number of memory access instructions, and (v) number of control flow instructions. Each core collects the telemetry independently and sends to the DQN module after every n (e.g., say $n=10,000$) instructions. When DQN module receives telemetry of at least a total of N (e.g., say, $N=500,000$) instructions, FORECASTER assumes the start of a new interval. DQN module aggregates the telemetry and normalizes each counter with respect to the total instructions of the interval that just finished. DQN module predicts the new configuration and sends a reconfiguration message to each core.

4.3 ISA Extension

We extend the ISA with instructions to set and get DQN configurations. We propose a fixed format for DQN configurations. The format is as follows - `<BOC>, Layer1, Layer2, ..., LayerN, <EOL>, Weight1, Weight2, ..., WeightM, <EOW>, LearningRate, DiscountFactor, ExplorationRatio, <EOC>`. Here, `<BOC>`, `<EOL>`, `<EOW>`, `<EOC>` are special markers (values) to indicate the beginning of configuration, end of layers, end of weights, and end of configurations respectively. We propose two instructions - `setconf %ri, %rc` and `getconf %rc, %ri`. `setconf %rc, %ri` sets the configuration value at address `[%ri]` into the configuration register `%rc`. On the other hand, `getconf %rc, %ri` reads from the configuration register `%rc` into the address `[%ri]`. In order to initialize the DQN module with a particular configuration, FORECASTER needs to invoke a function that executes a sequence of `setconf` instructions in a loop until `<EOC>`

marker is reached. Similarly, in order to save the current configuration of the DQN module, FORECASTER executes a sequence of `getconf` instructions in a loop until `<EOC>` marker is reached.

5. EXPERIMENTAL EVALUATION

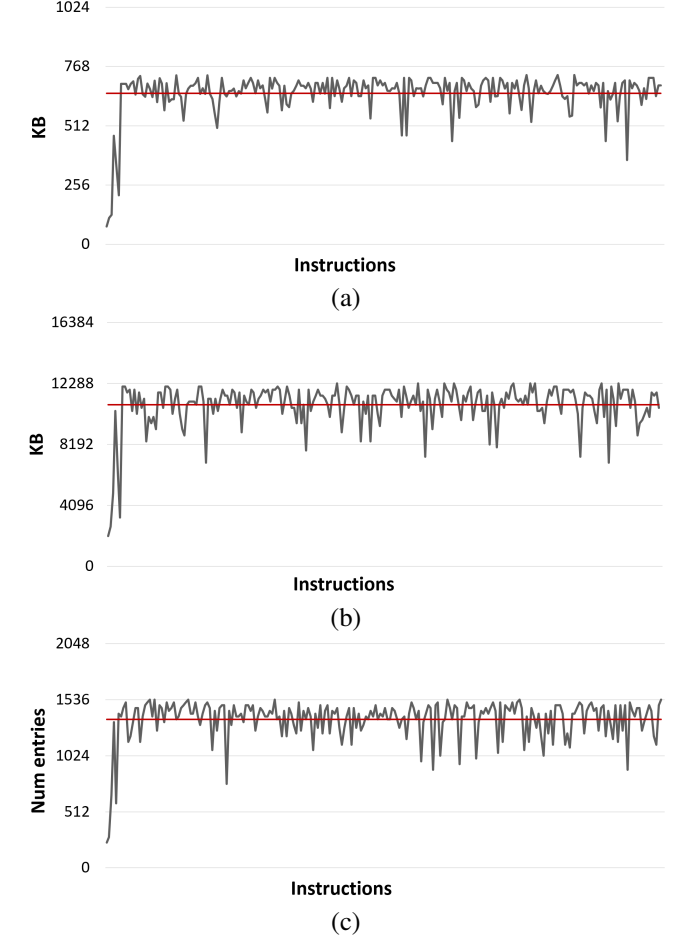


Figure 7: Avg amount of (a) L2, (b) L3, and (c) BTB turned off during the execution of *streamcluster*.

5.1 Experimental Setup

Table 2 shows the parameters of the simulated hardware that we use to conduct the experiments. We use a modified version of Multi2Sim [32] and McPAT [15] to simulate the experimental hardware and its power consumption. PARSEC 3.0 benchmark suite is used with small inputs. Due to resource and time constraints, all benchmarks are run to completion or 1 billion instructions. The interval size N is set at 0.5M instructions.

We conduct three experiments on three versions of FORECASTER:

- Experiment 1: FORECASTER is implemented with a giant table to store and update the Q-values. All applications are run five times. Each run starts with an empty Q-table. This version is essentially an adoption

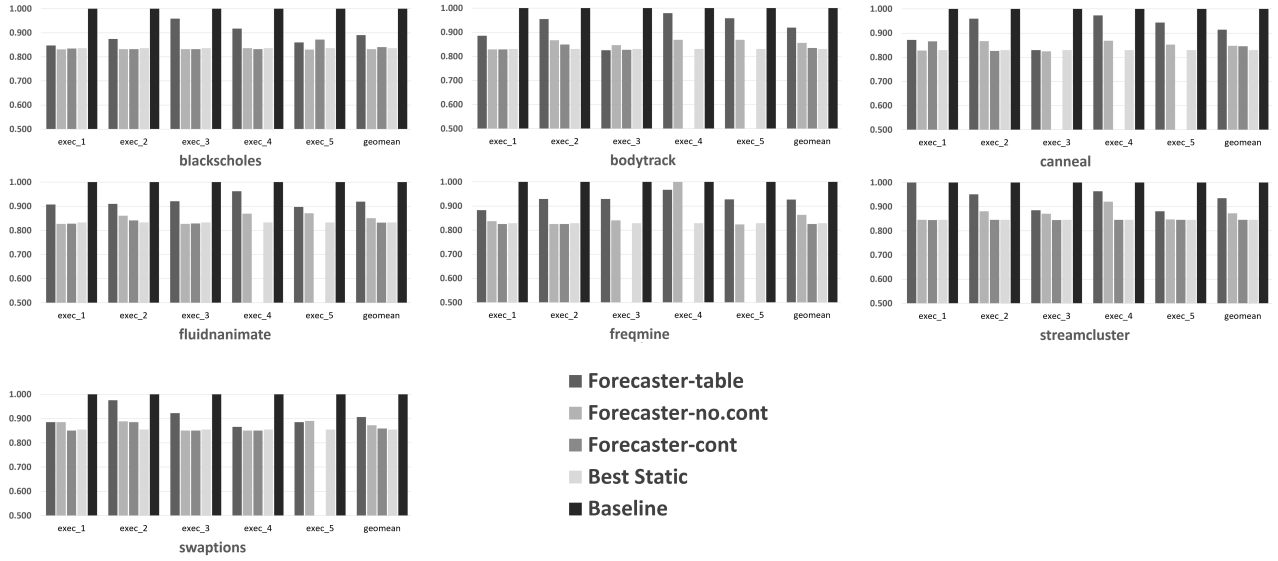


Figure 8: Normalized power consumption of five executions of applications

Parameter	Value
CPU	8-core @ 2.4Ghz, SMT off
Private L1 cache (I/D)	32KB, 64B line, 8-way
Private L2 Cache	1024K, 64B line, 8-way
Shared L3 Cache	16M, 64B line, 16-way
Coherence Protocol	Directory-based MOESI

Table 2: Parameters of the simulated hardware.

of prior reinforcement learning-based approach in the current usage scenario [12].

- Experiment 2: FORECASTER is implemented with a deep neural network to predict the Q-values. All applications are run five times. Each run starts with an untrained neural model.
- Experiment 3: FORECASTER is implemented with a deep neural network to predict the Q-values. All applications are run five times. Each run starts with the trained neural model inherited from the previous execution.

In the first experiment, each run starts with an empty Q-table, which means there is no knowledge accumulation between executions. This technique is basically the Q-learning adopted from [12]. In the second experiment, we replace the Q-table with a deep neural network to see how good DQN is compared to the vanilla Q-learning. Experiment 3 is similar to experiment 2 except an execution starts with the model taken from the previous execution. The purpose of this experiment is to investigate the efficacy of knowledge accumulation.

5.2 Results

5.2.1 In-flight Analysis

Figures 5(a), 5(b), 5(c) show how FORECASTER manages the hardware resources during an execution of *streamcluster*. On average, FORECASTER can turn off 64%, 66%, 66% L2 cache, L3 cache and the BTB respectively. FORECASTER also deactivates the prefetcher for 26% of all intervals. Similar behavior can be seen for other programs in the benchmark suite. FORECASTER is able to determine the best size for each structure for each phase. This can be seen from the repetitive pattern in the figures, which maps to phases in each program. In this paper, we use static phases, fixed number of instructions. In the future, we plan to use phase detection techniques [7, 26] and this is expected to make the scheme even more efficient.

5.2.2 Power Consumption

Experimental results shows that FORECASTER with continuous learning uses the least power compared to other techniques and similar to the best static configuration, as shown in Figure 8. On average, FORECASTER with accumulated knowledge can save 16% of power across all applications compared to the baseline. This is a 2% more than the version without continuous learning and 8% more than the version with basic Q-table.

5.2.3 Efficiency

The efficiency of each experiment is shown in Figure 9. In general, our scheme outperforms the baseline configuration in all benchmarks except from *canneal*. Interestingly, the Q-table version gives the best efficiency compared to the other two versions with the neural network. This may be because the Q-table does not require much time to learn compared to the neural network. Due to the time constraint, only two executions of *canneal* are completed for experiment 3. That is why the neural network does not perform as expected.

5.2.4 Performance

Figure 10 shows that there is not much IPC degradation when using FORECASTER. Specifically, the system IPC when

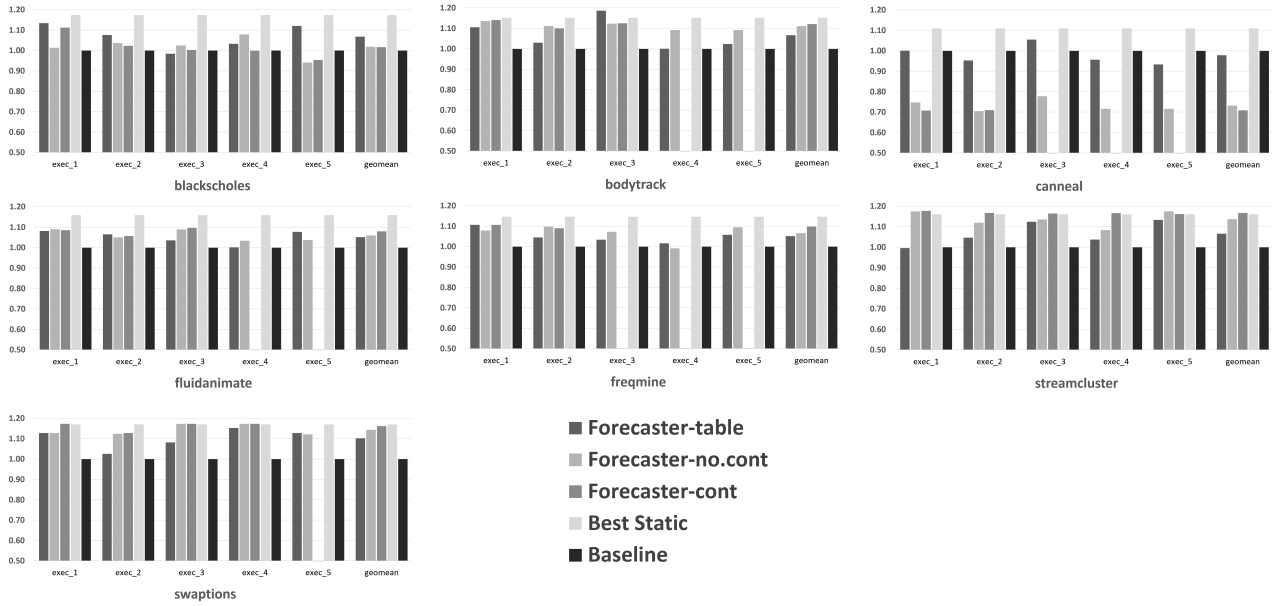


Figure 9: Normalized efficiencies of five executions of applications

running *swaption* is virtually unchanged across all version of FORECASTER. The Q-table version of FORECASTER has the most consistent performance as it only cause a 1.2% IPC overhead on average. This result is comparable to the best static configuration. In *canneal*, two versions with the deep neural network performs badly as they degrade the system IPC by about 15%. One reason is because it takes time to train the neural network before it can have reasonable accuracy.

The normalized execution time measured in terms of number of cycles is shown in Figure 11. In overall, the execution time overhead incurred by FORECASTER is less than 5%. FORECASTER tends to perform better in multi-threaded applications as seen in *streamcluster*, *swaptions*, *fluidanimate* compared to single-threaded applications such as *canneal*. This is because FORECASTER only makes one prediction for all cores, and the prediction is largely dependent on the resource of the core that is heavily used. For example, single threaded programs only use one core, therefore the L2 cache of that core is mostly occupied. However, when FORECASTER reconfigure the hardware, it turns off the same amount of L2 cache on every core, even though L2 caches on other cores are mostly empty. This is a limitation of FORECASTER that can be the subject of a future research.

5.2.5 Cost

The cost of the proposed design can be divided into three parts: delay or latency cost, hardware cost, and power consumption cost. As for the latency cost, reading the hardware telemetry and making a reconfiguration decision does not happen in the critical path. The hardware will continue in its old configuration till the decision is made for a new configuration.

The hardware cost consists of the DQN hardware and the extra hardware used to implement the knobs. The DQN uses a seven-layer neural network with six neurons per layer. There is also an input layer of 10 neurons and an output layer of one

neuron. So, we use eight processing elements to implement the input-layer, in two cycles as it needs to do the work of 10 neurons, and then one-cycle per each layer. Each processing element (PE) is a simple execution unit that can do a fused multiply-add operation per cycle similar to the execution units found in traditional Graphics processing units (GPUs). The PEs are organized together in a design similar to the neural processing unit (NPU) described in [9]. We also need two extra registers for the old Q value and the new Q value (calculated by the neural network based on the reward). A simple computation unit is needed to calculate the new Q value as shown in Section 3.4.

The hardware needed for the knobs is straightforward. The prefetcher is just clock-gated as the knob is on/off. The BTB also uses clock-gating depending on the configuration. We have four configurations so a small 2x4 decoder will do the job as shown in the reconfiguration logic of Figure 3. Clock gating the cache ways is simplified by the fact that the way-reconfiguration logic, shown in Figure 4, never gates a valid entry so no change to the cache controller or coherence hardware. The way-reconfiguration logic is not complicated because it exploits the fact that large caches (such as L3) is usually partitioned. Therefore we have one logic circuitry per partition.

The power consumption of the above hardware is not high due to several factors. First, that extra hardware is activated only at the end of each program phase to make prediction and reconfigure the knobs. Second, the extra power consumption is much smaller than the power-saved by gating the reconfigured structures. Finally, there are several options to design the neural network ranging from executing it, as a software component, on a CPU or GPU, or designing it as digital ASIC [9], FPGA [14], or analog ASIC [5, 16]. Each approach has its own characteristics of area, power, and cost.

5.2.6 Sensitivity Analysis

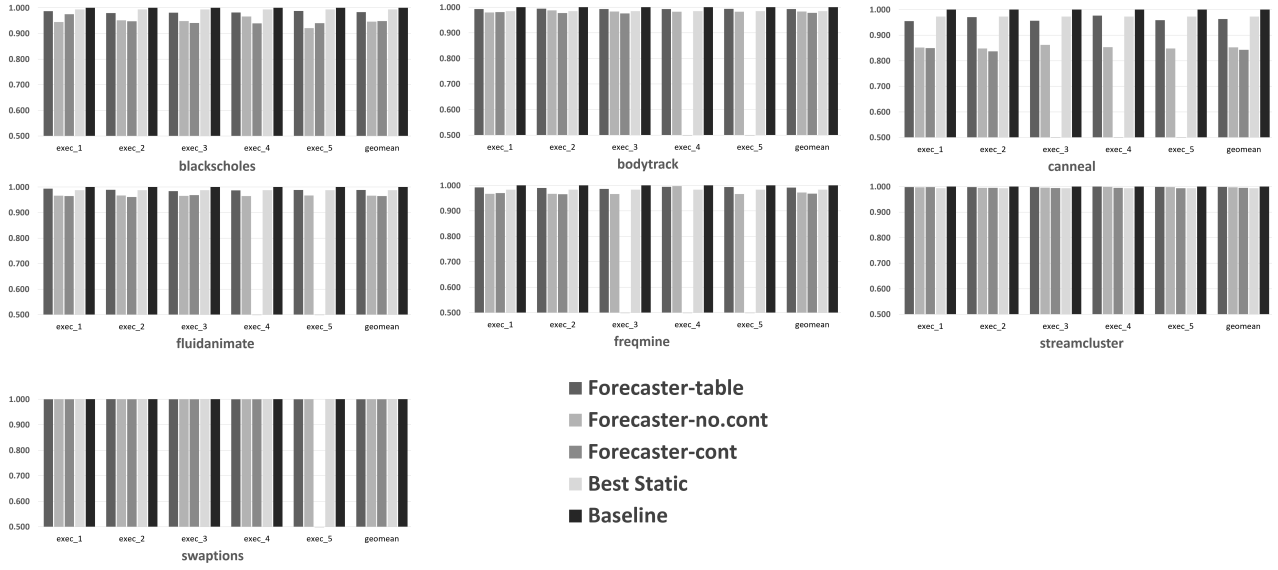


Figure 10: Normalized IPCs of five executions of applications

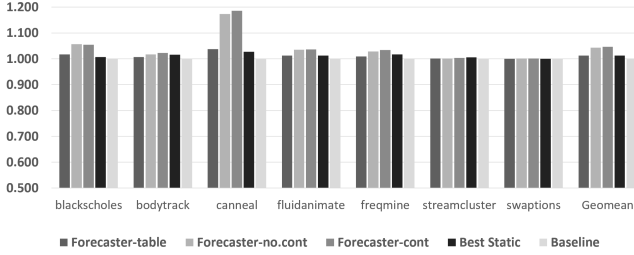


Figure 11: Normalized number of cycles taken between experiments

We conduct three additional experiments in order to determine the optimal interval size, history length, and number of counters to collect. The history length experiment shows how long into the past should we take into account for determining the best configuration of the current interval. Simulation results show that increasing the history length from 1 to 2 intervals reduces the efficiency gains by 3% as shown in Figure 12.

The number of counters experiment shows how many counters should be considered to best represent an interval. We test with 3 sets: 3-counter, 5-counter and 8-counter sets. Below is the list of 8 counters that we are collecting:

- Normalized number of dispatched integer instructions.
- Normalized number of dispatched logic instructions
- Normalized number of dispatched floating point instructions.
- Normalized number of dispatched memory instructions.
- Normalized number of dispatched control instructions.
- Minimum free space across all L2 caches
- Free space of shared L3 cache

- Branch predictor misprediction rate.

8-counter set includes all of counters above. 5-counter set includes the normalized dispatched instructions, leaving out the last 3 counters. 3-counter set only includes the number of dispatched integer, memory and control instructions. Figure 13 shows that a set of 5 counters gives the best efficiency. A set of 3 counters does not have enough representation power while a full set of 8 counters is redundant.

The third experiment determines how big an interval size should be. We test with interval sizes of 0.25M, 0.5M, 1M, 2M instructions. Simulation results shows that setting interval size at 0.5M instructions gives 0.02%, 0.11%, and 0.11% more efficiency gain than 2M, 1M and 0.25M instructions, respectively.

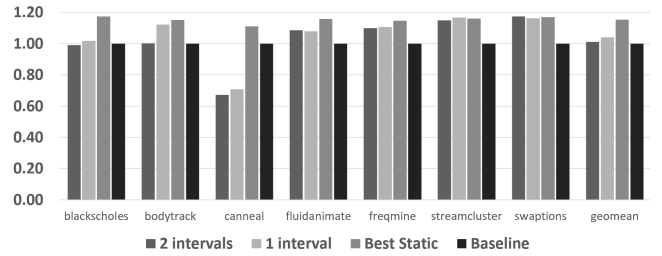


Figure 12: Efficiency comparison between different history lengths

5.2.7 Summary

In overall, the continuous learning version of FORECASTER can save up to 17.5% of power consumption in some applications and 16% on average compared to the baseline setup. It gives an efficiency gain of 4% while sacrificing 4.7% of execution time.

6. RELATED WORK

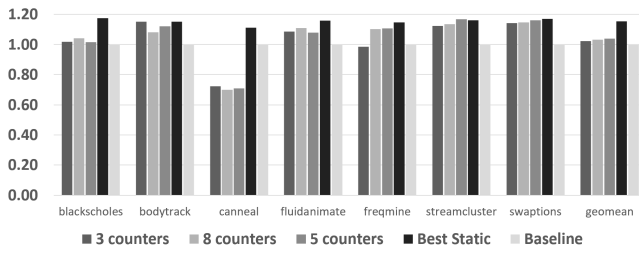


Figure 13: Efficiency comparison between different number of counters

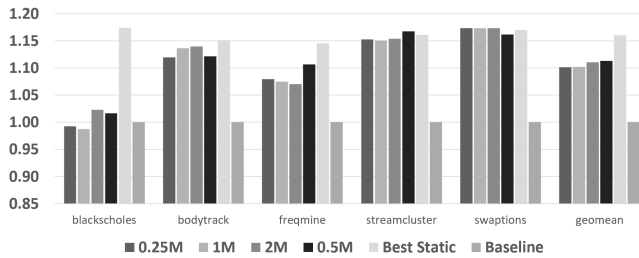


Figure 14: Efficiency comparison between different interval sizes

Tarsa et al. [31] propose a lightweight ML framework that can be distributed through firmware updates to the microcontroller for post-silicon CPUs. The ML model is first trained offline with a diverse collection of applications to avoid statistical blind spots. During execution, the CPU dynamically sets the issue width of a clustered hardware component while clock-gating unused resources based on the prediction of the ML model.

Pan et al. [20] present a multi-level reinforcement learning framework (MLRL) to address the scalability issue of the dynamic power management in multi-core processors. MLRL effectively reduce the exponential decision process into a linear problem by exploiting the hierarchical paradigm. In MLRL, core states and Q-values are propagated from the bottom to the top of the tree structure, then decisions are propagated back down the tree, providing an efficient control mechanism.

Ravi et al. [22] propose CHARSTAR, a clock tree aware resource optimizing mechanism. CHARSTAR incorporates a multi-layer perceptron with one hidden layer to predict the optimal configuration in each execution phase. The neural network takes into account the clock hierarchy and the topology overhead in order to improve the power savings. However, the offline trained model may soon be obsolete for future unmet programs. Secondly, CHARSTAR only works for single-threaded programs, and a multi-threaded version may cause a super-linearly increase in the size of the neural network model.

7. CONCLUSIONS

This work presents the potential of dynamically tuning hardware components to save power with a small performance overhead. Our scheme, FORECASTER, when incorporated a continuous learning deep neural network, can save up to 17.5% of power consumption compared to the base-

line configuration. On average, FORECASTER can reduce the power usage by 16% while sacrificing 4.7% of execution time, thus leads to a 4% efficiency gain. Future research may focus on improving the efficacy of Forecaster as well as extending the control of FORECASTER over more hardware resources to achieve more efficiency gain.

REFERENCES

- [1] M. Abadi, A. Agarwal, P. Barham, E. Brevdo, Z. Chen, C. Citro, G. S. Corrado, A. Davis, J. Dean, M. Devin, S. Ghemawat, I. Goodfellow, A. Harp, G. Irving, M. Isard, Y. Jia, R. Jozefowicz, L. Kaiser, M. Kudlur, J. Levenberg, D. Mané, R. Monga, S. Moore, D. Murray, C. Olah, M. Schuster, J. Shlens, B. Steiner, I. Sutskever, K. Talwar, P. Tucker, V. Vanhoucke, V. Vasudevan, F. Viégas, O. Vinyals, P. Warden, M. Wattenberg, M. Wicke, Y. Yu, and X. Zheng, "TensorFlow: Large-scale machine learning on heterogeneous systems," 2015, software available from tensorflow.org. [Online]. Available: <http://tensorflow.org/>
- [2] M. M. u. Alam and A. Muzahid, "Production-run software failure diagnosis via adaptive communication tracking," in *Proceedings of the 43rd International Symposium on Computer Architecture*, ser. ISCA '16. Piscataway, NJ, USA: IEEE Press, 2016, pp. 354–366. [Online]. Available: <https://doi.org/10.1109/ISCA.2016.39>
- [3] R. Balasubramanian, D. Albonese, A. Buyuktosunoglu, and S. Dwarkadas, "Memory hierarchy reconfiguration for energy and performance in general-purpose processor architectures," in *Proceedings of the 33rd Annual ACM/IEEE International Symposium on Microarchitecture*, ser. MICRO 33. New York, NY, USA: ACM, 2000, pp. 245–257. [Online]. Available: <http://doi.acm.org/10.1145/360128.360153>
- [4] R. Bitirgen, E. Ipek, and J. F. Martinez, "Coordinated management of multiple interacting resources in chip multiprocessors: A machine learning approach," in *Proceedings of the 41st Annual IEEE/ACM International Symposium on Microarchitecture*, ser. MICRO 41. Washington, DC, USA: IEEE Computer Society, 2008, pp. 318–329. [Online]. Available: <https://doi.org/10.1109/MICRO.2008.4771801>
- [5] V. Calayir, M. Darwish, J. Weldon, and L. Pileggi, "Analog neuromorphic computing enabled by multi-gate programmable resistive devices," in *Proceedings of the 2015 Design, Automation & Test in Europe Conference & Exhibition*, ser. DATE '15. San Jose, CA, USA: EDA Consortium, 2015, p. 928–931.
- [6] S. Choi and D. Yeung, "Learning-based smt processor resource distribution via hill-climbing," in *33rd International Symposium on Computer Architecture (ISCA'06)*, Jun 2006, p. 239–251.
- [7] A. S. Dhodapkar and J. E. Smith, "Managing multi-configuration hardware via dynamic working set analysis," in *Proc. 17th International Symposium on Computer Architecture*, 2002.
- [8] C. Dubach, T. M. Jones, E. V. Bonilla, and M. F. P. O'Boyle, "A predictive model for dynamic microarchitectural adaptivity control," in *2010 43rd Annual IEEE/ACM International Symposium on Microarchitecture*, Dec 2010, pp. 485–496.
- [9] H. Esmailzadeh, A. Sampson, L. Ceze, and D. Burger, "Neural acceleration for general-purpose approximate programs," in *Proceedings of the 2012 45th Annual IEEE/ACM International Symposium on Microarchitecture*, ser. MICRO-45. Washington, DC, USA: IEEE Computer Society, 2012, pp. 449–460. [Online]. Available: <https://doi.org/10.1109/MICRO.2012.48>
- [10] L. Graesser and W. L. Keng, *Foundations of Deep Reinforcement Learning: Theory and Practice in Python*. Boston, MA, USA: Addison-Wesley Professional, 2018.
- [11] H. Hubert and B. Stabernack, "Profiling-based hardware/software co-exploration for the design of video coding architectures," in *IEEE Transactions on Circuits and Systems for Video Technology*, Sep 2009, pp. 1680 – 1691.
- [12] E. Ipek, O. Mutlu, J. F. Martínez, and R. Caruana, "Self-optimizing memory controllers: A reinforcement learning approach," in *Proceedings of the 35th Annual International Symposium on Computer Architecture*, ser. ISCA '08. Washington, DC, USA: IEEE Computer Society, 2008, pp. 39–50. [Online]. Available: <https://doi.org/10.1109/ISCA.2008.21>
- [13] C. Isci, A. Buyuktosunoglu, C. Cher, P. Bose, and M. Martonosi, "An

- analysis of efficient multi-core global power management policies: Maximizing performance for a given power budget,” in *2006 39th Annual IEEE/ACM International Symposium on Microarchitecture (MICRO’06)*, 2006, pp. 347–358.
- [14] M.-J. Li, A.-H. Li, Y.-J. Huang, and S.-I. Chu, “Implementation of deep reinforcement learning,” in *Proceedings of the 2019 2nd International Conference on Information Science and Systems*, ser. ICISS 2019. New York, NY, USA: Association for Computing Machinery, 2019, p. 232–236. [Online]. Available: <https://doi.org/10.1145/3322645.3322693>
- [15] S. Li, H. Ann, R. D. Strong, J. B. Brockman, D. M. Tullsen, and N. P. Jouppi, “Mcpat: An integrated power, area, and timing modeling framework for multicore and manycore architectures,” in *2009 42nd Annual IEEE/ACM International Symposium on Microarchitecture (MICRO)*, Oct 2009, pp. 469–480.
- [16] D. Maliuk and Y. Makris, “An analog non-volatile neural network platform for prototyping rf bist solutions,” in *Proceedings of the Conference on Design, Automation & Test in Europe*, ser. DATE –14. Leuven, BEL: European Design and Automation Association, 2014.
- [17] V. Mnih, K. Kavukcuoglu, and D. Silver, “Human-level control through deep reinforcement learning,” in *Nature*, vol. 518, Feb 2015, p. 529–533.
- [18] V. Nair and G. E. Hinton, “Rectified linear units improve restricted boltzmann machines,” in *Proceedings of the 27th International Conference on International Conference on Machine Learning*, ser. ICML–10. Madison, WI, USA: Omnipress, 2010, p. 807–814.
- [19] D. Novillo, “Samplepro - the power of profile guided optimizations without the usability burden,” in *2014 LLVM Compiler Infrastructure in HPC*, Nov 2014, p. 22–28.
- [20] G.-Y. Pan, J.-Y. Jou, and B.-C. Lai, “Scalable power management using multilevel reinforcement learning for multiprocessors,” *ACM Trans. Des. Autom. Electron. Syst.*, vol. 19, no. 4, Aug. 2014. [Online]. Available: <https://doi.org/10.1145/2629486>
- [21] P. Petrica, A. M. Izraelevitz, D. H. Albonesi, and C. A. Shoemaker, “Flicker: A dynamically adaptive architecture for power limited multicore systems,” in *Proceedings of the 40th Annual International Symposium on Computer Architecture*, ser. ISCA ’13. New York, NY, USA: ACM, 2013, pp. 13–23. [Online]. Available: <http://doi.acm.org/10.1145/2485922.2485924>
- [22] G. S. Ravi and M. H. Lipasti, “Charstar: Clock hierarchy aware resource scaling in tiled architectures,” in *Proceedings of the 44th Annual International Symposium on Computer Architecture*, ser. ISCA –17. New York, NY, USA: Association for Computing Machinery, 2017, p. 147–160. [Online]. Available: <https://doi.org/10.1145/3079856.3080212>
- [23] B. Reagen, P. Whatmough, R. Adolf, S. Rama, H. Lee, S. K. Lee, J. M. Hernandez-Lobato, G.-Y. Wei, and D. Brooks, “Minerva: Enabling low-power, highly-accurate deep neural network accelerators,” in *International Symposium on Computer Architecture (ISCA)*, 2016. [Online]. Available: http://vlsiarch.eecs.harvard.edu/wp-content/uploads/2016/05/reagen_isca16.pdf
- [24] M. Riedmiller, R. Hafner, T. Lampe, M. Neunert, J. Degraeve, T. van de Wiele, V. Mnih, N. Heess, and J. T. Springenberg, “Learning by playing solving sparse reward tasks from scratch,” in *Proceedings of the 35th International Conference on Machine Learning*, ser. Proceedings of Machine Learning Research, J. Dy and A. Krause, Eds., vol. 80. Stockholm, Sweden: PMLR, 10–15 Jul 2018, pp. 4344–4353. [Online]. Available: <http://proceedings.mlr.press/v80/riedmiller18a.html>
- [25] T. Sherwood, E. Perelman, and B. Calder, “Basic block distribution analysis to find periodic behavior and simulation points in applications,” in *Proceedings of the 2001 International Conference on Parallel Architectures and Compilation Techniques*, ser. PACT –01. USA: IEEE Computer Society, 2001, p. 3–14.
- [26] T. Sherwood, S. Sair, and B. Calder, “Phase tracking and prediction,” *SIGARCH Comput. Archit. News*, vol. 31, no. 2, p. 336–349, May 2003. [Online]. Available: <https://doi.org/10.1145/871656.859657>
- [27] D. Silver, A. Huang, C. J. Maddison, A. Guez, L. Sifre, G. van den Driessche, J. Schrittwieser, I. Antonoglou, V. Panneershelvam, M. Lanctot, S. Dieleman, D. Grewe, J. Nham, N. Kalchbrenner, I. Sutskever, T. P. Lillicrap, M. Leach, K. Kavukcuoglu, T. Graepel, and D. Hassabis, “Mastering the game of go with deep neural networks and tree search,” *Nature*, vol. 529, pp. 484–489, 2016.
- [28] D. Silver, T. Hubert, J. Schrittwieser, I. Antonoglou, M. Lai, A. Guez, M. Lanctot, L. Sifre, D. Kumaran, T. Graepel, T. Lillicrap, K. Simonyan, and D. Hassabis, “A general reinforcement learning algorithm that masters chess, shogi, and go through self-play,” *Science*, vol. 362, no. 6419, pp. 1140–1144, 2018. [Online]. Available: <https://science.sciencemag.org/content/362/6419/1140>
- [29] D. Silver, J. Schrittwieser, K. Simonyan, I. Antonoglou, A. Huang, A. Guez, T. Hubert, L. R. Baker, M. Lai, A. Bolton, Y. Chen, T. P. Lillicrap, F. Hui, L. Sifre, G. van den Driessche, T. Graepel, and D. Hassabis, “Mastering the game of go without human knowledge,” *Nature*, vol. 550, pp. 354–359, 2017.
- [30] R. S. Sutton and A. G. Barto, *Reinforcement Learning: An Introduction*. Cambridge, MA, USA: A Bradford Book, 2018.
- [31] S. J. Tarsa, R. B. R. Chowdhury, J. Sebot, G. Chinya, J. Gaur, K. Sankaranarayanan, C.-K. Lin, R. Chappell, R. Singhal, and H. Wang, “Post-silicon cpu adaptation made practical using machine learning,” in *Proceedings of the 46th International Symposium on Computer Architecture*, ser. ISCA –19. New York, NY, USA: Association for Computing Machinery, 2019, p. 14–26. [Online]. Available: <https://doi.org/10.1145/3307650.3322267>
- [32] R. Ubal, J. Sahuquillo, S. Petit, and P. Lopez, “Multi2sim: A simulation framework to evaluate multicore-multithreaded processors,” in *19th International Symposium on Computer Architecture and High Performance Computing*, Oct 2007, pp. 62–68.
- [33] J. Wildstrom, P. Stone, E. Witchel, and M. Dahlin, “Machine learning for on-line hardware reconfiguration,” in *IJCAI 2007, Proceedings of the 20th International Joint Conference on Artificial Intelligence, Hyderabad, India, January 6-12, 2007*, 2007, pp. 1113–1118. [Online]. Available: <http://ijcai.org/Proceedings/07/Papers/180.pdf>